

**UNCLASSIFIED**

**AD 431 182**

**DEFENSE DOCUMENTATION CENTER**

**FOR**

**SCIENTIFIC AND TECHNICAL INFORMATION**

**CAMERON STATION, ALEXANDRIA, VIRGINIA**



**UNCLASSIFIED**

NOTICE: When government or other drawings, specifications or other data are used for any purpose other than in connection with a definitely related government procurement operation, the U. S. Government thereby incurs no responsibility, nor any obligation whatsoever; and the fact that the Government may have formulated, furnished, or in any way supplied the said drawings, specifications, or other data is not to be regarded by implication or otherwise as in any manner licensing the holder or any other person or corporation, or conveying any rights or permission to manufacture, use or sell any patented invention that may in any way be related thereto.

64-9

431182

AFCRL-64-38

*Final Report*

# **SOLUBILITY OF METAL OXIDES IN SUPERCRITICAL AQUEOUS SOLUTIONS**

*Prepared for:*

AIR FORCE CAMBRIDGE RESEARCH LABORATORIES  
OFFICE OF AEROSPACE RESEARCH  
UNITED STATES AIR FORCE  
BEDFORD, MASSACHUSETTS

CONTRACT NO. AF 19(628)-392  
PROJECT NO. 4608, TASK NO. 460805

No.

STANFORD RESEARCH INSTITUTE

MENLO PARK, CALIFORNIA



431182

DT DDC  
MAP 11/19/64  
JAN 1965

Requests for additional copies by Agencies of the Department of Defense, their contractors, and other Government agencies should be directed to the:

DEFENSE DOCUMENTATION CENTER (DDC)  
CAMERON STATION  
ALEXANDRIA, VIRGINIA

Department of Defense contractors must be established for DDC services or have their "need-to-know" certified by the cognizant military agency of their project or contract.

All other persons and organizations should apply to the:

U.S. DEPARTMENT OF COMMERCE  
OFFICE OF TECHNICAL SERVICES  
WASHINGTON 25, D.C.

STANFORD RESEARCH INSTITUTE

MENLO PARK, CALIFORNIA



AFCRL-64-38

*Final Report*

*For Period June 1, 1962 to October 31, 1963*

**SOLUBILITY OF METAL OXIDES IN SUPERCRITICAL AQUEOUS SOLUTIONS**

*Prepared for:*

AIR FORCE CAMBRIDGE RESEARCH LABORATORIES  
OFFICE OF AEROSPACE RESEARCH  
UNITED STATES AIR FORCE  
BEDFORD, MASSACHUSETTS

CONTRACT NO. AF 19(628)-392  
PROJECT NO. 4608, TASK NO. 460805

By: W. J. Silva R. C. Smith, Jr.

SRI Project No. PAU-4117

Copy No. 84

## ABSTRACT

In this investigation an effort has been made to elucidate some of the basic processes underlying the growth of single crystals from hydrothermal solutions. To grow crystals by this means it is necessary to find a region where a) the crystal is stable, b) the solubility of the compound is sufficient, and c) supersaturation is neither too low nor too high for growth at a reasonable rate. The study chiefly concerns measurements of the solubility of rutile in supercritical water and basic media in the temperature range 375 to 525°C under solution pressures of 5000 to 33,000 psi. The laboratory equipment used in such measurements is described, and a method for measuring the equilibrium densities of the solutions is discussed. A fundamental equation is derived which, with the use of the Van't Hoff equation, permits calculation, from only a few measurements, of the solubility of metal oxides in basic hydrothermal solutions. Results of this work and recently published data on ZnO, Al<sub>2</sub>O<sub>3</sub>, and BeO are correlated and used to demonstrate the applicability of the equation.

## TABLE OF CONTENTS

	Page
ABSTRACT	ii
LIST OF ILLUSTRATIONS	iv
LIST OF TABLES	v
 I. INTRODUCTION	 1
II. HIGH PRESSURE FACILITIES, EQUIPMENT, AND DESCRIPTIVE APPLICATION OF EQUIPMENT	3
III. DETERMINATIONS OF SOLUTION DENSITIES	11
IV. $\text{TiO}_2$	18
A. Crystalline Rutile in Water	18
B. $\text{TiO}_2$ Powder in Water	19
C. The Solubility of Single Crystal Rutile in Basic Media	22
V. OTHER METAL OXIDES INVESTIGATED	25
A. MgO	25
B. $\text{Gd}_2\text{O}_3$	27
C. $\text{Fe}_2\text{O}_3$	27
D. $\text{MnO}_2$	27
VI. DISCUSSION AND CONCLUSIONS	29
ACKNOWLEDGMENTS	38
REFERENCES	39

## LIST OF ILLUSTRATIONS

		Page
Figure 1	High Pressure Barricade	4
Figure 2	Unit Sampling-Reactor for Operating Temperatures up to 500°C at Pressures up to 30,000 psi	5
Figure 3	Unit Sampling-Reactor Assembly in Barricade compartment	8
Figure 4	14 ml Capacity High Pressure Vessel with Supported Closure	9
Figure 5	High Pressure, High Temperature Spectrophotometric Cell	10
Figure 6	High Pressure Piston Gauge (Pneumatic) Calibrator, Fused Quartz Bourdon Tube Null Detector and High Temperature Pressure Transducer	12
Figure 7	Apparent Molar Solubility Dependence of Rutile on Base Concentration at Constant Temperature and Nearly Constant Pressure	33
Figure 8	Solubility Dependence of Metal Oxides on Base Concentration of Solvent at Constant Temperature	35
Figure 9	Observed Temperature Effect of Solubility for Rutile System	37



# LIST OF TABLES

Table		Page
I	Solubility of Rutile in Supercritical $H_2O$	20
II	Solubility of $TiO_2$ (Powdered Form) in Water	21
III	Solubility of $TiO_2$ (Rutile) in 0.1 N NaOH under Hydrothermal Conditions	23
IV	$TiO_2$ (Rutile) in 1 N NaOH, 5 N NaOH, and 5 m $NH_4Cl$ under Hydrothermal Conditions	24
V	Observed Solubilities of MgO in Supercritical Water	26
VI	Observed Solubility of $Mn_2O_3$ in Hydrothermal Solution	29

## INTRODUCTION

Technological advances have placed increasing demands on solid state materials. Present and potential uses of semiconductor, piezoelectric, electro-optical, optical, ferro- and ferri-magnetic, maser, laser, and other devices have created more stringent requirements for high-purity materials and high-quality crystals. There is a special need for large perfect crystals, a need which has become more acute with the advent of optical maser research.

Many materials in use and many whose potential has yet to be developed are available as relatively large crystals only from natural resources or by means of fusion, vapor-phase, or precipitation and recrystallization techniques in the laboratory. Since the size of natural crystals is limited, synthetic techniques must be used to increase the available size. Some compounds are not amenable to existing crystal growing methods because (1) they are not readily soluble in some suitable recrystallizing solvent under ordinary conditions; (2) they decompose or sublime below their melting point; (3) they undergo a phase transition below that temperature; or (4) they melt incongruently or react with the solvent. Furthermore, crystals grown at relatively high temperatures are usually strained and have a large number of dislocations and vacancies. However, by employing a combination of elevated temperature and high solvent pressure, crystals can be grown from solution which could not be practicably grown by other means. Crystals produced in this manner normally do not have the high degree of undesirable qualities usually encountered in crystals of high-temperature origin.

The solvent commonly used for crystal growth from high-temperature, high-pressure solution is water, because of its high solvating power (largely due to its small molecular size and very large dielectric constant) and chemical nonreactivity with the solute. The advantages of this process (the hydrothermal process) have been demonstrated by the successful growth of large, high-quality quartz crystals<sup>1</sup> as well as

crystals of  $\text{ZnO}$ ,<sup>2</sup>  $\text{Al}_2\text{O}_3$ ,<sup>3</sup> and others.<sup>4</sup> In general, the approach to hydrothermal crystal growth is to place a seed crystal in the upper part of an autoclave and raw material (nutrient) in the growth region under operating conditions. Temperatures usually of 400 to 500°C and solvent pressures up to 3000 atmospheres are employed with the upper part of the autoclave being some 10 to 50°C cooler than the bottom. Thus, the solution is saturated in respect to the solute, or nutrient, at the higher temperature but supersaturated at the lower temperature in the region of growth.

The feasibility of growing high-quality single crystals of a broad category of compounds suggests the importance of establishing some principles of hydrothermal crystal growth from which one may deduce, at least semiquantitatively, conditions conducive to growth of a particular crystal. Laudise<sup>4</sup> has proposed some qualitative and empirical guides for hydrothermal crystal growth based on his work with quartz and on other information. These guides present a good general basis, but a more refined treatment awaits a better understanding of the nature and behavior of aqueous solutions, and of the mechanisms of solution in the supercritical region. To develop such a treatment, basic information is required on the extent and rate of solubility of compounds in supercritical aqueous solutions and the dependence of these parameters on the very nature of the solute, and on the temperature, pressure, composition, and pH of the solution. This information is readily available for many compounds at room temperature and even up to 100°C; above this temperature data are scarce, particularly in the critical and supercritical region of water where the only comprehensive data, until very recently, were on  $\text{SiO}_2$ ,<sup>5-7</sup> (in the case of weak electrolytes) and some ionic salts such as  $\text{NaCl}$ ,<sup>8-10</sup>  $\text{KCl}$ ,<sup>11</sup>  $\text{HCl}$  and  $\text{KOH}$ .<sup>12</sup> Very recently data were published reporting the solubility of  $\text{ZnO}$ ,<sup>13</sup>  $\text{Al}_2\text{O}_3$ ,<sup>14</sup> and  $\text{BeO}$ <sup>15</sup> in basic hydrothermal solutions.

This research program was undertaken to obtain some of this vital information. The task of developing equipment and facilities was mainly performed during a previous contract, AF19(604)-5697, sponsored by AFCRL.

Under the present contract that task was completed and work performed included testing of equipment developed earlier, as well as designing and constructing some special high pressure equipment for AFCRL consisting of a spectrophotometric cell, a piston-gauge calibrator, and some strain-gauge pressure transducers. Solubility data were collected, primarily on  $\text{TiO}_2$ , as crystalline rutile. During the course of testing equipment and developing appropriate techniques for measuring the solubilities of these compounds, some fragmentary data were also obtained on  $\text{MnO}_2$ ,  $\text{MgO}$ , and  $\text{Fe}_2\text{O}_3$ . This information is discussed in this report along with a section describing measurements and calculations performed to obtain the densities of the saturated solutions. The conclusions derived from this work, which are supported by the recently published data on other metal oxides, help to elucidate some of the fundamental processes which occur in basic hydrothermal media.

## II HIGH PRESSURE FACILITIES, EQUIPMENT, AND DESCRIPTIVE APPLICATION OF EQUIPMENT

The basic high-pressure laboratory for hydrothermal solubility studies at Stanford Research Institute has previously been described in "AFCRL 51, Scientific Report No. 1," under AFCRL Contract No. AF19(604)-5697. During the course of the present contract the laboratory was expanded to accommodate new unit sampling-reactors and furnaces. A barricade which provides more than adequate protection was constructed from readily available 5/8-inch armor plate, lined with 1-inch plywood, to house the new units. All control, monitoring, and valve-actuator equipment was mounted on the outside of the barricade. The barricade, shown in Fig. 1, was designed to allow the autoclaves to be rolled in and out of the furnaces on carriages.

The autoclave, illustrated in Fig. 2, was designed for measuring solubilities by sampling the solution at equilibrium without perturbing the system. Three sampling chambers which are isolated by valves from



FIG. 1 HIGH PRESSURE BARRICADE

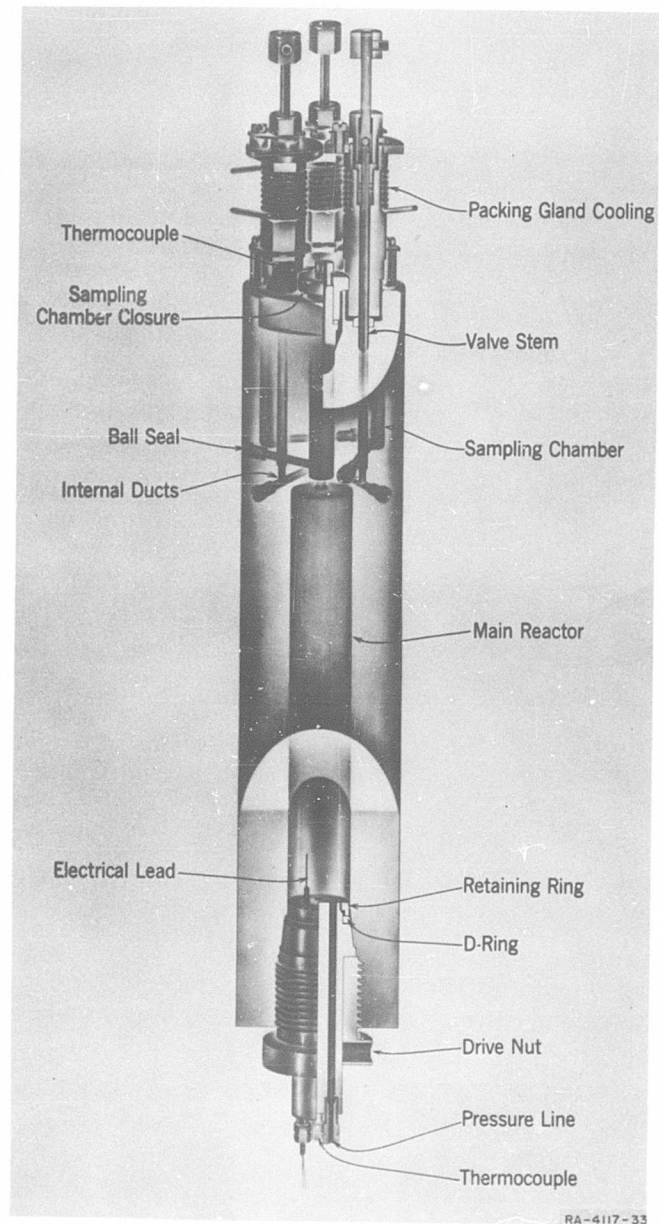


FIG. 2 UNIT SAMPLING-REACTOR FOR OPERATING TEMPERATURES UP TO 500°C AT PRESSURES UP TO 30,000 psi

the main chamber are embodied in the reactor. These permit samples of the solution to be collected at different time intervals (for establishing whether true equilibrium has been attained) under the same pressure and temperature conditions or at different temperatures and respective pressures but at constant density. The main closure on this vessel utilizes a "self-energizing" D-ring seal. The head of the vessel was designed to accommodate a pressure line to a pressure gauge or transducer, a thermocouple, and an electrical lead, for conductivity measurements. While in operation, water is circulated through cooling coils around the valve packing glands to prevent the Teflon packing from overheating. Two tools were machined for loosening the closures on the vessel: one for prying open the covers on the sampling chambers, the other a "jack" for loosening the drive nut on the main reactor closure at the conclusion of high temperature-high pressure runs.

For normal operation, the vessel was filled, sealed, and hydrostatically tested to 45,000 psi at room temperature. Since conductivity measurements were not attempted with these autoclaves, the port designed to accommodate an electrical lead was available for charging and discharging the sealed vessel. After hydrostatic testing, water was removed through this port until only sufficient water remained to produce the desired pressure at equilibrium. The powdered solute (in the case of  $\text{MgO}$ ,  $\text{Gd}_2\text{O}_3$ , and powdered  $\text{TiO}_2$ ) was then injected into the main chamber of the vessel through a 6-inch hypodermic needle. Care was taken, during this procedure, to keep the solute at the base of the vessel and not allow it to settle in the channel leading to the sampling chambers, in which case the resulting solubility data could have been fortuitously high. After this port was plugged, the vessel was evacuated to remove all free air. A valve inserted in the high pressure line leading to the pressure gauge was used to retain the vacuum. At the conclusion of the experiments, samples were collected from each sampling chamber and from the channels linking the chambers to their respective valves. Each solution was weighed (to obtain the solubility in terms of weight percent), combined with the rinse solutions, and prepared for analysis.

A furnace was fabricated on a Unistrut frame specifically for use with the unit sampling reactor. The furnace itself was built in the form a 3-foot-long cylinder,  $14\frac{1}{2}$  inches O.D., cut axially into two parts. Each part was mounted on the framework in such a way that it could swing through a  $30^\circ$  angle (from the edge of the frame to the center) and could be rotated  $180^\circ$  about its axis when unobstructed. With this type of construction the sampling reactor, on its carriage, could be rolled into the center of the furnace and the two furnace parts clamped together. Thermocouples were fastened at 6-inch intervals along the interior walls of the furnace, at a position corresponding to the center of each heating section of the furnace. Each of the five heating sections was provided with its own voltage regulator so that the temperature along the length of the furnace could be set for any desired operating condition. Water inlet and outlet manifolds were installed above the furnace for circulating water through the valve-cooling jackets of the reactor. A safety valve was connected in the water inlet line; if the water pressure should drop below a safe level, the solenoid on this valve would be activated and in turn switch off the power to the furnace. Valve extension shafts were also mounted to the framework. These shafts protruded through the top of the barricade and engaged with right-angle drives which were connected to the valve handles attached to the control panel. Figure 3 shows the arrangement of the reactor, carriage, and furnace situated in the barricade at the end of a typical experiment.

Six such furnaces and unit sampling-reactors were also constructed during this and the previous contract for Air Force Cambridge Research Laboratories.

Many experiments were conducted in autoclaves of the type illustrated in Fig. 4. This vessel is small (14 ml capacity), and is easily heated; its contents can be brought to equilibrium quickly, and the vessel is easier to handle than the large reactors. Although only one solubility measurement can be made with each experiment in these autoclaves (three measurements can be gathered from the unit sampling-reactors), the frequency of failure is relatively low. Solubilities were measured in



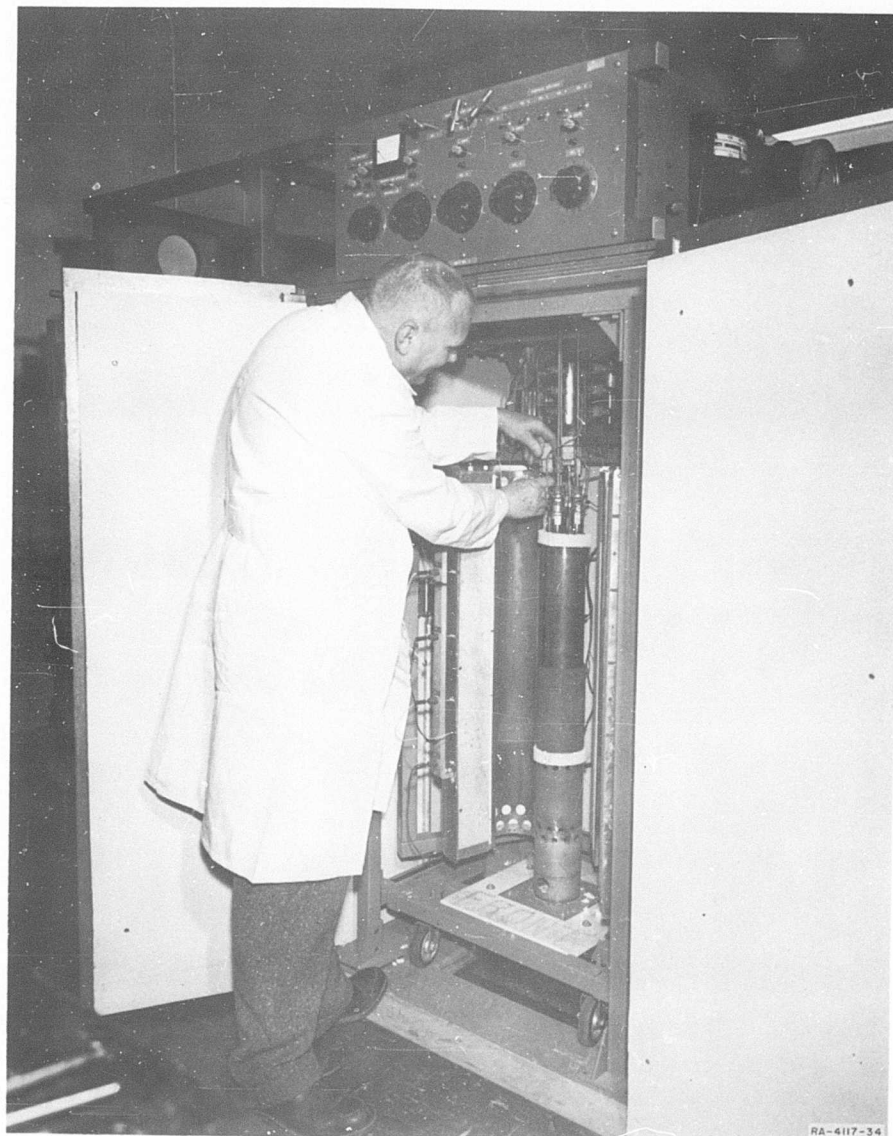


FIG. 3 UNIT SAMPLING-REACTOR ASSEMBLY IN BARRICADE COMPARTMENT

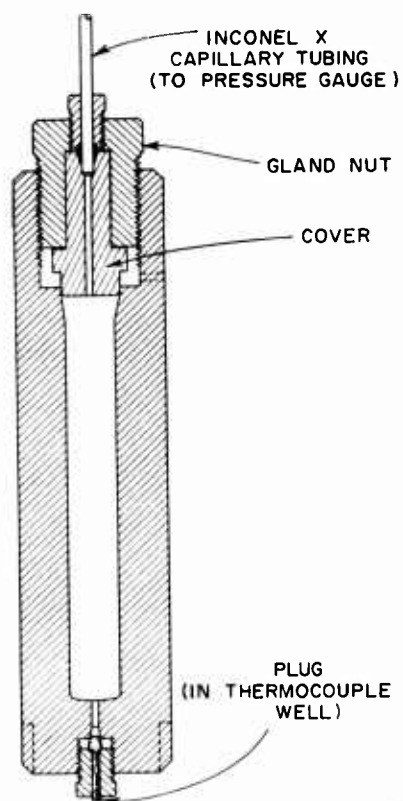


FIG. 4 14 ml CAPACITY HIGH PRESSURE VESSEL WITH SUPPORTED CLOSURE

these vessels by weight loss and sampling techniques. Sampling in this case was accomplished by inserting copper or stainless steel test tubes (depending on the nature of the solute and solvent) in the autoclaves above the solute. The sample recovered from the test tube is then the condensed phase of the total solution present at equilibrium, provided that the solute does not pass through a solubility maximum at some intermediate temperature and pressure. However, in this case all solubility values collected at temperatures above this maximum would be constant. Grain size of the solute in these experiments is critical, for fine powders can be circulated throughout the vessel and produce anomalous results.

A spectrophotometric cell, illustrated in Fig. 5, was designed and constructed for optical observation of species in aqueous solution at temperature up to 500°C and pressures up to 40,000 psi. This cell can be used with either quartz or sapphire windows (preferably sapphire with aqueous solutions above 425°C, because  $\text{Al}_2\text{O}_3$  is the stable phase<sup>16</sup> above this temperature and its solubility in water is less than

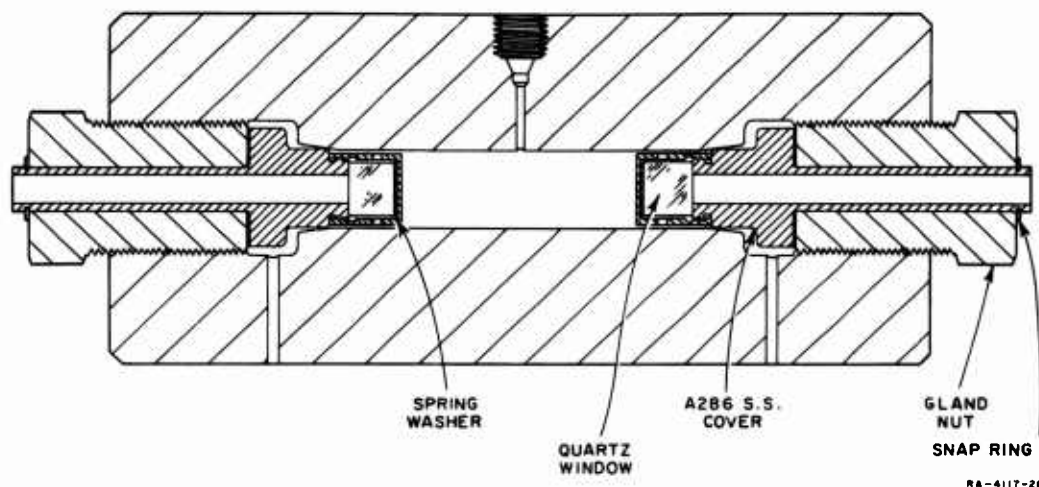


FIG. 5 HIGH PRESSURE, HIGH TEMPERATURE SPECTROPHOTOMETRIC CELL

one-thousandth that of quartz<sup>17</sup>) and is attached to the large reactor through a high temperature, high pressure valve. The seals are so designed that the cell can be evacuated at room temperature. Through a series of mirrors and light-shielding tubes, the solution is irradiated with monochromatic light through one window and the resulting radiation, emerging from the opposite window, is detected by a phototube. During an experiment the cell, which has been heated to the same temperature as the reactor, is filled with the solution from the reactor; the optical absorption of the solution is measured; and the cell is relieved of its contents by releasing the solution through a second valve into a collector.

A high-pressure calibrator, with some novel features was obtained primarily for use at AFCRL. This piston-gauge calibrator operates on a pressure balance principle. The force generated on the piston, by some hydrostatic pressure (up to 50,000 psi), is transmitted to a diaphragm. Since low gas pressures are used to balance the force on the piston, a

low pressure detector is sufficient for measuring the pressure. A very sensitive, highly accurate fused quartz Bourdon tube is employed in this capacity. Displacement of the Bourdon tube with pressure is detected by the degree of deflection of a mirror attached to the base of the tube. The degree of deflection is measured by a null detector equipped with a direct digital readout dial. The corresponding hydrostatic pressure is then obtained from a calibration curve for the observed null value.

The piston-gauge calibrator, shown in Fig. 6, is accurate to one part in 5000. Among its more desirable features is its weight (only 40-50 pounds) compared with conventional dead-weight testers. Thus it has the additional advantage of portability.

In the foreground of Fig. 6 is shown a high temperature, high pressure strain-gauge pressure transducer which was developed to measure the pressure of hydrothermal solutions. This device was designed to connect to the high pressure reactors within the furnace. The hydrothermal solution enters the front of the transducer and makes contact with a gold-lined diaphragm. The pressure of the solution is then transmitted from the diaphragm through the solid core of the transducer to the strain gauges. A water jacket surrounds the strain gauges to prevent the gauges from deviating from room temperature while water is circulating regardless of the temperature at the diaphragm. The voltage output of the transducer is linear with pressure and directly proportional to the input voltage at constant temperature.

### III DETERMINATIONS OF SOLUTION DENSITIES

Much of the work reported in the literature on hydrothermal solutions relates the dependence and character of the solute in solution as a function of temperature and pressure but neglects the effect of volume. The reason for this omission is understandable, for in some cases volumetric measurements are beyond the scope of the work and of no consequence to the object of the investigation. Even in cases where P-V-T data would

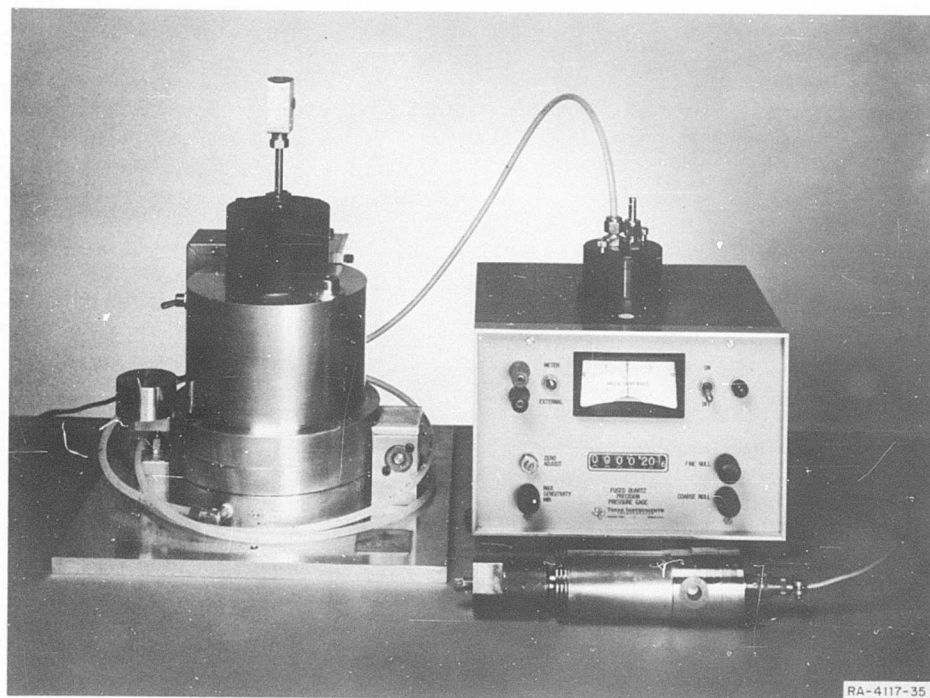


FIG. 6 HIGH PRESSURE PISTON GAUGE (PNEUMATIC) CALIBRATOR, FUSED QUARTZ BOURDON TUBE NULL DETECTOR AND HIGH TEMPERATURE PRESSURE TRANSDUCER (FOREGROUND)

contribute to an improved understanding of the study, the difficulties imposed by such measurements make them unfeasible or impractical to perform.

However, the object of this study is to contribute information from which a better understanding of hydrothermal solutions can be gained; hence, volumetric measurements are important. Since the masses of solvate and solvent are known, in solubility determinations, the equilibrium volume of the solution can be calculated directly from the equilibrium density of the solution.

First, consider the total experimental system at equilibrium, consisting of the autoclave, shown in Fig. 4, at a constant temperature,  $t_1$ , the pressure gauge at ambient temperature,  $t_0$ , and the connecting capillary line at temperature  $t_x$ , where  $t_x$  varies between  $t_0 \leq t_x \leq t_1$  along the length of the line. The whole system contains an internal pressure  $P_1$ .

The total volume of the system  $V_T$ , at  $P_1$ ,  $t_1$ , is the sum of (a) the initial volume of the autoclave  $V_{A_0}$ , (b) the initial volume of the gauge and line  $V_{GL_0}$ , (c) the pressure dilation of the autoclave  $\Delta V_A$ , and (d) the expansions due to pressure of the gauge  $\Delta V_G$  and of the line  $\Delta V_L$ :

$$V_{T_{P_1 t_1}} = V_{A_0} + V_{GL_0} + \Delta V_A + \Delta V_G + \Delta V_L$$

Similarly, the total mass of water in the system,  $m_T$ , is the sum of the mass in the autoclave,  $m_{1A}$ , the mass in the line,  $m_{1L}$ , and the mass in the gauge,  $m_{1G}$ :

$$m_{T_{P_1 t_1}} = m_{1A} + m_{1L} + m_{1G}$$

For experimental calculations, however, the P-V-T-m relationships within the isothermal confines of the autoclave are of primary importance. The volume of the autoclave  $V_1$ , at  $P_1$ ,  $t_1$ , is

$$V_1 = V_{A_0} + \Delta V_A,$$

and the mass of water within the autoclave,  $m_1$ , at  $P_1$ ,  $t_1$ , is

$$m_1 = m_{A_0} - \Delta m_G - \Delta m_L,$$

$\Delta m_G$  and  $\Delta m_L$  are the mass of water required to expand the gauge and line at pressure  $P_1$ . Therefore the specific volume of water within the autoclave  $V_{S_1}$ , at  $P_1$ ,  $t_1$ , is  $V_{S_1} = V_1/m_1$ . This value of  $V_{S_1}$  can be calculated from Holser and Kennedy's<sup>18, 19</sup> data for water once the experimental values of  $P_1$  and  $t_1$  have been measured.

Since

$$V_{S_1} = \frac{V_1}{m_1} = \frac{V_{A_0} + \Delta V_A}{m_{A_0} - \Delta m_G - \Delta m_L} \quad (1)$$

once  $\Delta V_A$  or  $\Delta m_G$  and  $\Delta m_L$  are determined as a function of temperature and pressure for a given system, then  $V_1$  or  $m_1$  can be calculated for any experiment performed within that system by measuring  $P_1$  and  $t_1$ .

To determine  $\Delta V_A$  accurately is difficult, for  $\Delta V_A$  is not easily separable from  $\Delta V_L$  with changing temperature and pressure. Also, not readily determinable is  $\Delta m_L$  which varies directly with pressure but inversely with temperature. The direct determination of these values can be eliminated by the following procedure.

As the volume of the autoclave expands, as a result of pressure dilation, from  $V_{A_0}$  to  $V_{A_0} + \Delta V_A$  the mass of water within the autoclave expands to occupy the new volume. This mass which occupies  $\Delta V_A$  is  $\Delta m_A$  and is related to  $\Delta V_A$  by the expression  $\Delta m_A = \frac{\Delta V_A}{V_{S_1}}$ .

The total loss of mass,  $\Delta m_1$ , from  $V_{A_0}$  at  $P_1$ ,  $t_1$  is therefore

$$\Delta m_1 = \Delta m_G + \Delta m_L + \Delta m_A$$

Inserting this into Eq. (1), we obtain

$$V_{S_1} = \frac{V_{A_0} + \Delta V_A}{m_{A_0} - \Delta m_1 + \Delta m_A}, \text{ which reduces to } V_{S_1} = \frac{V_{A_0}}{m_{A_0} - \Delta m_1} \quad (2)$$

where  $\Delta m_1 = m_{A_0} - m_1 + \Delta m_A$ .

Therefore, by measuring  $V_{A_0}$ ,  $m_{A_0}$ ,  $P_1$ , and  $t_1$  and calculating  $V_{S_1}$  from Holser and Kennedy's data we can compute  $\Delta m_1$ . This quantity can be determined as a function of temperature and pressure for each system; with its dependence upon  $P_1$  and  $t_1$  known,  $\Delta m_1$  for any solubility experiment can be calculated and the density of the solution computed as will be shown.

To obtain the variation of  $\Delta m_1$  over the experimental temperature and pressure range, P-T plots were drawn for each system from the experimental data obtained with water at percentage fills of 60, 70, and 80%. P-T couplets were obtained from the curves at temperatures corresponding to experimental temperatures at which the solubility data were acquired.  $V_S$  values were computed for the P-T couplets by cubic interpolation of Holser and Kennedy's data for water. Thus, from the measured quantities  $V_{A_0}$ ,  $m_{A_0}$ , and the computed values of  $V_{S_1}$ ,  $\Delta m_1$  was calculated from Eq. (2).

The volume,  $V_{A_0}$ , of each autoclave varies slightly from experiment to experiment due to variations in displacement of the cover upon sealing and the amount of CuO added to the autoclave.\* However, under similar conditions where  $P_1^a$ ,  $t_1^a$ ,  $V_{S_1}^a$ , =  $P_1^b$ ,  $t_1^b$ ,  $V_{S_1}^b$  and

$$\frac{V_{A_0}^a}{m_{A_0}^a} = \frac{V_{A_0}^b}{m_{A_0}^b}, \text{ it follows that } \frac{\Delta m_1^a}{m_{A_0}^a} = \frac{\Delta m_1^b}{m_{A_0}^b}. \text{ Therefore, } \Delta m_1/m_{A_0} \text{ versus}$$

---

\* CuO was placed in the autoclave to remove hydrogen formed by the dissociation of water and corrosion of the vessel by the supercritical steam. This step was taken to insure accurate agreement of the data with those of Holser and Kennedy.



pressure curves were plotted at specific temperatures (at 25°C intervals from 325° to 525°C) for each system. For application to the solubility experiments,  $\Delta m_1/m_{A_0}$  values were graphically interpolated along appropriate isotherms for the corresponding measured equilibrium pressures.

The validity of this argument was borne out in eight solubility experiments on crystalline rutile in which pure water was used as solvent. The solubility of rutile in water is so low it can be assumed that any electrostriction of the solvent, due to the solvated species, is negligible and well below the limits of experimental detection. From the observed equilibrium pressures and temperatures, the measured  $V_{A_0}$  and  $m_{A_0}$  values, and the  $\Delta m_1/m_{A_0}$  at  $P_1$ ,  $t_1$  for the system, the specific volumes,  $V_{S_1}$ , of the solutions (water) were calculated by means of Eq. (2). These values were then compared with Holser and Kennedy's data at the corresponding pressures and temperatures. The agreement was good. The mean deviation between the observed specific volumes and the specific volumes calculated from Kennedy's data was  $\pm .007$  cc/g, which represents a mean error of 0.4%. Maximum deviation for a single experiment was 0.025 cc/g which amounted to an error of 1.4%.

This method of determining densities was most usefully applied to solubility measurements in which the solute and solvent (1N or 5N NaOH) were encapsulated in platinum and the water in the autoclave provided mainly a pressure-supporting media for the capsule. In this case the specific volume calculated from Holser and Kennedy's data at  $P_1$ ,  $t_1$ ,

$$V_{S_1} = \frac{V_{A_0} - V_{cap}}{m_{A_0} - \Delta m_1}$$

where the volume of the capsule at equilibrium,

$V_{cap} = V_{platinum} + V_{crystal} + V_{solution}$ . Thus from the final weight and the density of the crystal, the mass and density of the platinum,  $V_{platinum}$  and  $V_{crystal}$ , were calculated. The volume of the solution is then the calculated volume of the capsule minus these two quantities.

The density of the solution at equilibrium is then

$$\rho_{\text{sol}}_{p_1, t_1} = \frac{\text{mass of solvent} + \text{mass of dissolved solute}}{V_{\text{solution}}}$$

Experimentally, to provide the highest degree of accuracy and reproducibility in density measurements under these conditions, the gauge and connecting line of each system were evacuated and filled with water under vacuum prior to each run. The sealing surfaces of the autoclaves were polished and the vessels cleaned. After the autoclaves were sealed, with test tubes in them, they were evacuated and filled with water under vacuum. The weight of the water reservoir (a polyethylene bottle) was measured before and after filling the autoclave and the temperature of the water recorded. The volume of water required to fill the autoclave was then calculated. The distance from the top of the main gland nut to the top of the autoclave body was measured. This distance was again measured after the final sealing of the vessel to determine the volume correction to be applied (arising from the slight displacement of the cover from sealing to sealing). With experiments containing platinum capsules this whole procedure was repeated, with the filled and sealed capsule in the autoclave. From this second volume measurement, the mass of water added to give the desired degree of fill was calculated. In such experiments the initial volume measurement was made on the empty autoclave. From the initial measured volume of the autoclave and the volume of CuO added (calculated from its mass and density),  $V_{A_0}$  for the autoclave was calculated. By rigorous adherence to this procedure,  $V_{A_0}$  was measured to within  $\pm 0.002$  ml.

The mass of water,  $m_{A_0}$ , added to the autoclave was less accurately known, for it was introduced into the autoclave with a volumetric pipette which could be read only to 0.01 ml. However, a check of the accuracy of the experiments showed that this mass determination (as calculated from the volume and respective density of water) was sufficient for these density measurements.

All experimental high temperatures were recorded and specific values were read off the recorder chart paper. The recorders were calibrated with a potentiometer and temperatures were found reproducible within  $\pm 1^\circ\text{C}$ . All chromel-alumel thermocouples, used to measure the temperature of the autoclaves, were calibrated against a Pt-Pt-10% Rh thermocouple standardized by the National Bureau of Standards. Although these thermocouples were strapped to the outer skin of the autoclaves (at the center), earlier experiments with thermocouples both inside and outside the vessels showed that once thermal equilibrium had been established in the furnace, the temperature on the outer skin of the vessel was in all cases within  $1^\circ\text{C}$  of the internal temperature.

Each pressure gauge was calibrated with respect to a standard 0-50,000 psi Heise gauge. Pressure deviations were plotted at 2,500 psi intervals and corrections interpolated from the graph. The average mean pressure deviation, for all gauges, was within  $\pm 50$  psi.

#### IV $\text{TiO}_2$

##### A. Crystalline Rutile in Water

A rutile boule, obtained from Linde Company, was sawed and cleaved to produce many small (0.1 to 0.2 gram) single crystals which were used in all the solubility measurements reported in this section.

Solubility experiments in conductivity water were prepared by placing a weighed rutile crystal in a clean autoclave (of the type illustrated in Fig. 4) and a clean stainless steel test tube of 4 ml capacity above the crystal. The test tube was covered with a 325-mesh stainless steel screen to prevent coarse powder from contaminating the contents of the test tube in the event the crystal fractured. A predetermined quantity of conductivity water was then added to the autoclave from a volumetric pipette. The temperature of the water was recorded for the calculation of its mass,  $m_{\text{A}_0}$ . The autoclave was sealed and placed in the furnace after the necessary steps were completed for density measurements. All experiments were

allowed to remain at equilibrium for at least 24 hours and some were maintained at equilibrium for periods up to 3 weeks. At the end of each experiment the contents of the test tube were weighed and the test tube rinsed three times with concentrated  $\text{H}_2\text{SO}_4$  to dissolve any  $\text{TiO}_2$  which may have precipitated as the solution condensed. The solution and rinses were then submitted for quantitative analysis. The rutile crystal was also weighed at the end of each experiment to determine whether it had lost any weight. The interior of the autoclave and the test tube were rinsed with concentrated sulphuric acid to remove all traces of  $\text{TiO}_2$ , in preparation for the next experiment. The results of these experiments are presented in Table I.

Table I shows that in the region  $375^\circ$  to  $525^\circ\text{C}$  and 5000 to 33,000 psi the effect of high temperature and pressure does not increase the molar solubility of rutile in supercritical water to a value of even  $2.5 \times 10^{-5}$  moles/liter. The data reported at  $385^\circ\text{C}$  and  $510^\circ\text{C}$  were obtained from solubility measurements conducted in a large (285 ml capacity) autoclave, similar to the one illustrated in Fig. 2 but without the sampling compartments. Rutile crystals were suspended in the autoclaves containing conductivity water and the vessels were thus heated to temperature and allowed to remain there for one week. At the end of the experiment the crystals were weighed to determine any weight loss, and the solution and rinse from each vessel were combined for analysis. The analytically determined quantities of  $\text{TiO}_2$  were used for calculating the reported solubilities, since the weight loss of the crystals was below the sensitivity of the analytical balance and thus not measurable.

#### B. $\text{TiO}_2$ Powder in Water

In some early solubility experiments on  $\text{TiO}_2$ , measurements were carried out exactly as described above with the exception that pressed  $\text{TiO}_2$  powder was used as solute in place of rutile crystals and copper test tubes were used as the sample collectors. Solubilities, calculated from the analytically determined quantities of  $\text{TiO}_2$  in solution and the masses of the respective solutions, are listed in Table II.

Table I

SOLUBILITY OF RUTILE IN SUPERCRITICAL H<sub>2</sub>O

Temperature °C	Pressure psi	Equilibrium Density of Solution g/cc	Solubility	
			wt % g/100 g	S moles/liter
375	4,800	0.58	$< 3.3 \times 10^{-4}$	$< 2.4 \times 10^{-5}$
375	8,950	0.67	$< 2.7 \times 10^{-4}$	$< 2.3 \times 10^{-5}$
375	17,900	0.76	$< 2.4 \times 10^{-4}$	$< 2.3 \times 10^{-5}$
† 385	33,500	0.87	$9.3 \times 10^{-6}$	$1.0 \times 10^{-6}$
425	10,100	0.58	$< 3.5 \times 10^{-4}$	$< 2.5 \times 10^{-5}$
425	14,400	0.66	$< 2.7 \times 10^{-4}$	$< 2.2 \times 10^{-5}$
425	26,400	0.78	$< 2.4 \times 10^{-4}$	$< 2.3 \times 10^{-5}$
475	14,300	0.57	$< 3.5 \times 10^{-4}$	$< 2.5 \times 10^{-5}$
475	20,250	0.65	$< 2.9 \times 10^{-4}$	$< 2.3 \times 10^{-5}$
475	31,100	0.73	$< 2.5 \times 10^{-4}$	$< 2.3 \times 10^{-5}$
500	32,900	0.73	$< 2.6 \times 10^{-4}$	$< 2.3 \times 10^{-5}$
† 510	30,750	--	$1.3 \times 10^{-5}$	$1.2 \times 10^{-6}$
520	18,000	--	$< 4.6 \times 10^{-3}$	---
525	17,450	0.55	$< 3.7 \times 10^{-4}$	$< 2.5 \times 10^{-5}$
525	27,950	0.66	$< 2.9 \times 10^{-4}$	$< 2.5 \times 10^{-5}$
575	27,150	--	$< 3.0 \times 10^{-4}$	$< 2.5 \times 10^{-5}$

† Equilibrium volume of solution was 285 ml.

Table II  
SOLUBILITY OF  $\text{TiO}_2$  (POWDERED FORM) IN WATER

Temperature °C	Pressure psi	Solubility Wt %
320	30,050	$7.2 \times 10^{-4}$
450	31,250	$3.0 \times 10^{-3}$
470	18,900	$1.0 \times 10^{-3}$
475	13,900	$7.7 \times 10^{-3}$
505	23,200	$9.1 \times 10^{-3}$

The solubility values appear high in comparison with the data for rutile in pure water; higher in fact than one would anticipate from surface area considerations alone. It is known that relatively large concentrations of cupric ions in solution may interfere with the spectrophotometric analysis for titanium; even though the peaks for the two ions are well separated, the copper band could overlap the titanium band resulting in an additive effect. It is suspected that the 475°C measurement is high due to this interference of copper. However, the  $\text{Cu}^{\text{II}}$  concentration, in general, was low and should have had negligible (or no) effect on the other analytical results.

A primary factor in the solubility of  $\text{TiO}_2$  in water arises from its crystal structure. The powder used in these experiments was that of brookite and not rutile. According to Pauling<sup>20</sup> the presence of shared edges and particularly shared faces in a coordinated crystal structure decreases its stability; this effect is more prominent with cations of high valence and small ligancy. This effect is produced by the greater proximity of the cations in these structures resulting in increased cationic repulsive forces. In rutile the octahedra share two edges, in anatase three, and in brookite four. Therefore, the solubility of rutile in water is expected to be less than for anatase and considerably less

than for brookite. In view of this, the data in Table II are considered representative for the solubility of brookite in water under the stated conditions of temperature and pressure.

C. The Solubility of Single Crystal Rutile in Basic Media

The solubility of rutile was measured in 0.1 N, 1.0 N, and 5.0 N (6.67m) NaOH solutions. Experiments with 0.1 N NaOH were performed in the same manner as those in water. The rutile crystals were all darkened during the experiments presumably from the diffusion of iron (arising from corrosion of the autoclaves) into the crystals. X-ray analysis showed that the rutile had not transformed to anatase and was not reduced by hydrogen during the experiments. Traces of contaminants were evident but unidentifiable.

Measurements in more basic solution were conducted within sealed platinum capsules. The weighed crystal was placed in a platinum test tube of known internal volume, and the test tube filled with solvent to the same degree of fill as the autoclave. The test tube was sealed by welding either by torch or by means of a cold pressure weld (difficulties encountered in sealing the test tubes with a torch made it necessary to find a simpler and more satisfactory method for sealing). Weights of the test tube -- empty, before filling, and after, and at the end of the experiment, before and after emptying -- were obtained so that the mass of solvent and solution was known at each step of the experiment. The capsule was placed in the autoclave, shown in Fig. 4, the latter containing a weighed mass of CuO, and the vessel was then filled to the desired level with water. All experiments were allowed to remain at equilibrium temperature and pressure for at least 12 hours and in most cases 24 hours. Temperature and pressure were measured as accurately as possible for density determinations. The crystals were weighed after all precipitate had been removed from their surfaces; this required scraping sodium titanate from the surfaces of each crystal.

The molar concentration of  $\text{TiO}_2$  in 0.1 N NaOH solution and the weight percent solubility of  $\text{TiO}_2$ , in grams of  $\text{TiO}_2$  per 100 grams of solution,

at equilibrium, are presented in Table III along with the density of the saturated solution at equilibrium pressure and temperature.

Table III  
SOLUBILITY OF  $\text{TiO}_2$  (RUTILE) IN 0.1 N NaOH UNDER HYDROTHERMAL CONDITIONS

Temperature °C	Pressure psi	Density of Solution g/cc	Solubility	
			wt. %	moles/liter
375	4,800	0.58	$< 3.4 \times 10^{-4}$	$< 2.5 \times 10^{-5}$
375	7,600	0.68	$1.2 \times 10^{-5}$	$1.0 \times 10^{-4}$
375	18,500	0.76	$3.4 \times 10^{-3}$	$3.2 \times 10^{-4}$
425	9,600	0.57	$8.0 \times 10^{-4}$	$5.7 \times 10^{-5}$
425	15,000	0.67	$1.1 \times 10^{-3}$	$9.4 \times 10^{-5}$
425	18,600	--	$7.2 \times 10^{-4}$	$6.9 \times 10^{-5}$
475	14,050	0.56	$5.1 \times 10^{-4}$	$3.6 \times 10^{-5}$
475	14,550	--	$5.2 \times 10^{-4}$	---
475	19,850	0.65	$8.7 \times 10^{-4}$	$7.1 \times 10^{-5}$
475	29,000	0.73	$5.6 \times 10^{-4}$	$5.1 \times 10^{-5}$
525	18,400	0.55	$1.7 \times 10^{-3}$	$1.2 \times 10^{-4}$
525	24,600	0.65	$5.4 \times 10^{-3}$	$4.4 \times 10^{-4}$

Table IV lists the results of the measurements in 1 N NaOH, 5 N NaOH and the single solubility measurement in 5 m  $\text{NH}_4\text{Cl}$ . With some experiments the formation of a yellow compound was noticed; in some cases the solution was discolored, in others either the crystal was coated with the compound or only a trace of the compound was observed in the normally white precipitate. X-ray analysis of this compound revealed that  $\text{Na}_2\text{O} \cdot 5 \text{TiO}_2$  was being formed. The conditions at which formation of this species was observed are listed in the table. In all other 1 N NaOH and 5 N NaOH solutions the principal species formed was  $\text{Na}_2\text{O} \cdot 3 \text{TiO}_2$ , as detected by X-ray analysis of the precipitates. In view of the sodium titanate formation, results of the measurements are reported in weight percent only; i.e., grams of  $\text{TiO}_2$  (as measured by the weight loss of the crystal) per 100 grams of solution.



Table IV

$\text{TiO}_2$  (RUTILE) IN 1 N NaOH, 5 N NaOH, AND 5 m  $\text{NH}_4\text{Cl}$   
UNDER HYDROTHERMAL CONDITIONS

Solvent	Temperature °C	Pressure psi	Density of Solution g/cc	Wt. % $\text{TiO}_2$	$\text{Na}_2\text{O} \cdot 5 \text{TiO}_2^*$ Formation	Equilibrating Period
1 N NaOH	375	4,400	0.60	$2.9 \times 10^{-1}$	No	20 hrs.
"	375	15,900	0.82	$1.3 \times 10^{-2}$	Trace	17 hrs.
1 N NaOH	400	16,100	0.79	$4.5 \times 10^{-2}$	Trace	18 hrs.
"	425	8,200	0.63	$3.0 \times 10^{-1}$	Yes	16 hrs.
"	437	14,400	0.73	$7.1 \times 10^{-1}$	Yes	24 hrs.
1 N NaOH	475	13,200	0.65	$4.8 \times 10^{-1}$	No	13 hrs.
1 N NaOH	525	17,600	0.66	1.01	Trace	13 hrs.
"	525	24,600	--	1.41	No	15 hrs.
1 N NaOH	~ 550	~28,000	--	3.7	---	---
4 N NaOH	375	4,000	0.71	0.66	No	23 hrs.
5 N NaOH	375	8,050	0.93	0.85	Trace	12 hrs.
"	375	12,900	0.97	1.80	No	15½ hrs.
5 N NaOH	425	10,600	0.92	0.78	Trace	22 hrs.
5 N NaOH	525	16,250	--	3.0	No	17½ hrs.
"	525	20,950	0.94	2.0	No	29 hrs.
5 m $\text{NH}_4\text{Cl}$	425	7,300	0.96	$<2.3 \times 10^{-3}$	---	24 hrs.

\* Principal species in 1 N and 5 N NaOH was  $\text{Na}_2\text{O} \cdot 3 \text{TiO}_2$

Two rate-of-solution experiments were performed in 5 N NaOH at 425°C. The autoclaves were placed in the hot furnace and brought to temperature. At the end of 5 and 10 minutes, respectively, the power to the furnace was turned off and the autoclaves showered with water from water lines which had previously been installed at the top of the furnace. By this method complete quenching was effected within 6 minutes. Quantitative results from these experiments were unreliable because the seals on the platinum capsules did not remain secure during the whole run. However, a qualitative evaluation of the results indicated that approximately

40% of the equilibrium value had been achieved after 5 minutes and 60% after 10 minutes, considering the 16-hour equilibrium solution as 100%.

## V OTHER METAL OXIDES INVESTIGATED

### A. MgO

The phase diagram of the  $\text{MgO-H}_2\text{O}$  system has been studied quite extensively.<sup>21-24</sup> At temperatures up to  $600^\circ\text{C}$  and pressures above the critical pressure of  $\text{H}_2\text{O}$ ,  $\text{Mg}(\text{OH})_2$  is the stable form of  $\text{MgO}$  in water and  $\text{MgO}$  undergoes complete hydrolysis under these conditions. The weight loss method, understandably, cannot be applied to solubility measurements in this region, but the solubility temperature and pressure dependence of the hydroxide is important for crystal growth applications. For, presumably, if the solubility of the hydroxide is appreciable below the transition temperature, growth could occur by keeping the seed crystal above this temperature and the nutrient below, provided of course (a) that the crystal can be isolated from the solution while heating to temperature, and (b) that the system is pressure-quenched at the end of the experiment.

Solubilities of  $\text{MgO}$  in water ( $\text{Mg}(\text{OH})_2$ ) were measured in three ways. One method employed the use of the unit sampling-reactor, shown in Figs. 2 and 3; another technique was to sample by test tube, as previously described. Both methods produced similar results; i.e., a wide scatter of the data. With  $\text{MgO}$ , whether introduced as the powder directly, or as a pressed pellet, the hydrolyzed particles are so fine that they are readily agitated throughout the solution by convection currents. This effect was somewhat enhanced in the unit sampling-reactors because of the heat distribution throughout the vessel, produced by valve-cooling jackets, and resulting in strong convection currents.

A third sampling method was similar to the test tube technique, except that the solute was placed in the test tube and the solution collected in the autoclave. This procedure offered the advantage that convection currents were virtually nonexistent in the test tube and that equilibrium

was established more likely by diffusion than convection stirring. This method is expected to be more reliable than the other two. The solubility data calculated from the experiments are listed in Table V along with the method employed to collect the samples; SR denotes the unit sampling-reactor, tt the test-tube technique, and AC the method of sampling with the autoclave from the solute containing test tube. The lowest value of each set is probably more representative of the solubility of  $\text{Mg}(\text{OH})_2$  under the stated conditions.

Table V  
OBSERVED SOLUBILITIES OF  $\text{MgO}$  IN SUPERCRITICAL WATER

Temperature °C	Pressure psi	Solubility Wt. %	Sampling Method
410	16,300	$2.6 \times 10^{-4}$	AC
480	8,000	$6.8 \times 10^{-3}$	SR
480	8,000	$1.0 \times 10^{-4}$	SR
480	8,000	$4.4 \times 10^{-3}$	SR
480	8,000	$3.0 \times 10^{-3}$	tt
480	8,000	$1.5 \times 10^{-3}$	tt
480	8,000	$2.4 \times 10^{-4}$	tt
480	20,300	$6.0 \times 10^{-5}$	SR
490	21,500	$7.3 \times 10^{-5}$	SR
495	22,000	$3.3 \times 10^{-3}$	SR
515	17,500	$2.3 \times 10^{-4}$	AC
515	17,500	$2.7 \times 10^{-4}$	AC
515	17,500	$8.2 \times 10^{-4}$	tt
520	13,900	$5.2 \times 10^{-4}$	Perturbation *
525	6,600	$1.7 \times 10^{-2}$	tt
525	6,600	$1.0 \times 10^{-2}$	tt
525	6,600	$1.2 \times 10^{-3}$	tt

\* Single experiment in which sampling autoclave was separated from large autoclave through valve and capillary tubing. At equilibrium valve was opened, sample collected, and valve closed again.

B. Gd<sub>2</sub>O<sub>3</sub>

Gadolinium oxide was studied in the same manner as MgO in a unit sampling-reactor. The results were very unfavorable; for example, from three samples which were collected together under the same conditions from one experiment, no precipitate was observed in one sampling chamber, some oxide was observed in the second, and an abundance of Gd<sub>2</sub>O<sub>3</sub> was visibly detected in the third chamber. This same behavior was observed with MgO in one experiment performed in the unit sampling-reactor. Unfortunately, time limitations prohibited further work on this investigation.

C. Fe<sub>2</sub>O<sub>3</sub>

Solubility studies on Fe<sub>2</sub>O<sub>3</sub> in H<sub>2</sub>O were hindered by the formation of Fe<sub>3</sub>O<sub>4</sub> resulting from the solute and corrosion products of the autoclave. A single investigation on the change of capacitance of the saturated solution indicated that Fe<sub>2</sub>O<sub>3</sub> is present in colloidal suspension at temperatures up to 385°C.

D. MnO<sub>2</sub>

Coarse manganese dioxide powder was employed as solute in these experiments. The relatively large grain size of the powder made it suitable for use in weight loss experiments. The fact that MnO<sub>2</sub> does not hydrolyze extensively in the temperature pressure region investigated made it additionally adaptable to this technique. A container for the solute was fabricated from 325 mesh stainless steel wire cloth. Experiments were performed in the autoclave by the weight loss method and by the test tube sampling technique. Platinum test tubes were substituted for stainless steel because hydrogen peroxide was required to remove the precipitate from the test tubes.

Results of the weight loss method are not reported because the solubility measurements were impaired by the reduction of MnO<sub>2</sub> as evidenced from X-ray analysis of the products deposited on the walls of the autoclaves. Thus, the values were high because this technique measures not

only the amount of solute lost by way of solvation but also the amount lost due to reaction.

Since platinum test tubes were used for solubility measurements, no reactions were expected to occur which would have been promoted by the material of which the test tubes were composed. Reductions taking place within the test tubes would occur only as a result of free hydrogen or some other mild reducing agent which was produced by reaction at or near the walls of the autoclave. It is therefore assumed that a saturated solution and no excess solute existed within the test tube at equilibrium. However, the species in solution within the test tube at equilibrium is believed to have been solvated  $\text{Mn}_2\text{O}_3$ . Upon entering solution  $\text{MnO}_2$  was reduced to  $\text{Mn}_2\text{O}_3$  and it is believed that this reaction proceeded to completion, i.e., equilibrium was established only after the solution became saturated and the excess  $\text{MnO}_2$  powder was covered with a layer of precipitated  $\text{Mn}_2\text{O}_3$  (contaminated with  $\text{Fe}_2\text{O}_3$ ) preventing the further dissolution of  $\text{MnO}_2$ . Again, evidence of this reduction is based on the X-ray analysis of products formed in other experiments. The product was either  $\text{Mn}_2\text{O}_3$  or  $(\text{Mn}, \text{Fe})_2\text{O}_3$  but manganese was present as the trivalent oxide.

At the conclusion of an earlier experiment, in which copper test tubes were inserted in a large autoclave to collect samples of the solution, a thick layer of  $\text{CuO}$  crystals was observed on the surface of the  $\text{MnO}_2$ .  $\text{CuO}$  crystals were not formed in experiments with other solutes, for  $\text{CuO}$  itself is a relatively strong oxidizing agent in hydrothermal media and is normally converted to  $\text{Cu}_2\text{O}$  and copper during the course of an experiment. Because  $\text{MnO}_2$  either oxidized copper to  $\text{Cu}_2\text{O}$  and  $\text{CuO}$  or prevented  $\text{CuO}$  from being reduced by hydrogen shows that  $\text{MnO}_2$  is a stronger oxidizing agent, under similar conditions. Furthermore, this oxidizing power of  $\text{MnO}_2$  indicates that (1) all solvated  $\text{MnO}_2$  is probably reduced under hydrothermal conditions, and (2) the solutions in the platinum test tubes were saturated with  $\text{Mn}_2\text{O}_3$  and not  $\text{MnO}_2$ . The data reported in Table VI then are believed to represent the solubility

of  $\text{Mn}_2\text{O}_3$  under the stated conditions and have been calculated on the basis of the molecular weight of that compound; however, the evidence that the species was  $\text{Mn}_2\text{O}_3$  and solely  $\text{Mn}_2\text{O}_3$  is not conclusive.

Table VI  
OBSERVED SOLUBILITY OF  $\text{Mn}_2\text{O}_3$  IN HYDROTHERMAL SOLUTION

Solvent	Temperature °C	Pressure psi	Solubility Wt %
$\text{H}_2\text{O}$	475	13,450	$< 7 \times 10^{-5}$
0.1 N NaOH	375	2,250	$< 8 \times 10^{-5}$
"	375	3,000	$< 6 \times 10^{-5}$
0.1 N NaOH	425	4,800	$5.0 \times 10^{-4}$
0.1 N NaOH	525	8,050	$4.1 \times 10^{-4}$

## VI DISCUSSION AND CONCLUSIONS

As mentioned in Part I, Laudise<sup>4</sup> has reported the fundamental empirical and qualitative rules for crystal growth from hydrothermal solutions. The basic conditions as reported by Laudise are:

1. A combination of solvent, pressure and temperature must be discovered in which the crystal is thermodynamically stable and has sufficient solubility to permit a reasonable supersaturation so that appreciable rates of crystallization can be obtained without excessive wall or homogeneous nucleation. For substances so far studied, solubilities of 2 to 5% are generally required.\*
2. Sufficiently large values of the ratio of the surface area of nutrient to the surface area of seeds that dissolving is not rate limiting.

\* 2 to 3 wt % solubility has been found to be sufficient.

3. Sufficiently large  $(\partial\rho/\partial t)_{\bar{\rho}}$ , temperature coefficient of solution density at constant  $\bar{\rho}$  average solution density so that with an appropriate temperature differential the convective circulation will be sufficiently rapid not to be rate-limiting.
4. Temperature coefficient of solubility  $(\partial s/\partial t)_p$  such that an appropriate temperature differential will produce a satisfactory supersaturation.\*\*
5. Vessel suitable to contain the pressure-temperature conditions of the experiment without excessive corrosion.

Thus, we see that in terms of growing single crystals of any specific compound from hydrothermal solution the primary factors which must be considered are (a) the stability of the compound in a hydrothermal media, and (b) the solubility of the compound. If the stability of the compound is not known from phase diagrams, it can be studied simultaneously with solubility determinations in water by quenching the solution at the end of an experiment and analyzing the products.

The approximate solubility of a compound in water at high temperatures and high pressures can be calculated from Franck's<sup>25</sup> relationship

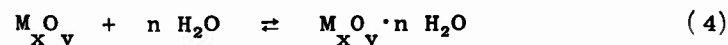
$$\ln \frac{X_2}{X_2^0} \simeq \frac{V_{2f}P}{RT} + n \ln \frac{K_{21}}{V} \quad (3)$$

provided the ambient solubility of the compound is known, as well as its association number and association constant. In his treatment, Franck has related the solubility not only to temperature and pressure but also to the molar volume of the solute,  $V_{2f}$ , the molar volume of the solvent,  $V$  (more accurately, the molar volume of the solution, but for dilute solutions the volume of the solvent can be inserted as a first approximation), the association number  $n$ , and the association constant  $K_{21}$ .

---

\*\* About 0.1 wt % supersaturation appears to be sufficient, since excessive supersaturation produces spontaneous nucleation in the growth region and insufficient supersaturation reduces the growth rate considerably.

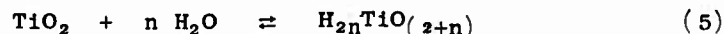
for the equilibrium reaction



Application of Eq. (3), even as a first approximation to the solubility of a compound, normally requires a solubility measurement at some elevated temperature and pressure, for  $n$  and  $K$  are not frequently known. Morey and Hesselgesser's<sup>17</sup> solubility data for several compounds at 500°C and 15,000 psi may be of help in determining  $n$  and  $K$  for the reported materials.

It is interesting to note that while the solubilities of the compounds investigated by Morey and Hesselgesser ranged from 0.2 part per million for  $\text{UO}_2$  to 2600 ppm for  $\text{SiO}_2$ , rutile exhibits the lowest solubility of all in water. The solubility of rutile in ppm at 500°C and 15,000 psi is about 0.01.

Let us now consider the probable mechanism of solution of rutile in water. As  $\text{TiO}_2$  dissolves in water the hydrated species hydrolyzes, according to Eq. (4):



The weak acid  $\text{H}_4\text{TiO}_4$  is known to exist at room temperature along with other products of hydrolysis. The equilibrium constant for Eq. (5) would then be

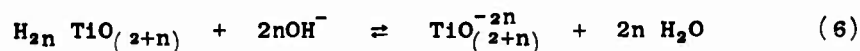
$$K_H = \frac{\text{H}_{2n} \text{TiO}_{(2+n)}}{\text{TiO}_2} = \frac{\text{H}_4\text{TiO}_4}{\text{TiO}_2}$$

for the known titanate acid, following the convention of omitting  $\text{H}_2\text{O}$  from the equilibrium equation since the concentration of water is virtually constant. Since the concentration of  $\text{TiO}_2$  is constant, as long as the solid is present, the constant of hydrolysis is equal to the molal solubility of the titanate, or

$$K_H = \text{H}_{2n} \text{TiO}_{(2+n)} .$$



When a base is added to the solution the acid is neutralized and equilibrium again is established:



The equilibrium constant for Eq. (6) is

$$K' = \frac{[\text{TiO}_{(2+n)}^{-2n}]}{[\text{H}_{2n} \text{TiO}_{(2+n)}][\text{OH}^-]^{2n}}$$

The two constants can then be combined to form the expression

$$[\text{OH}^-]^{2n} = \frac{[\text{TiO}_{(2+n)}^{-2n}]}{K_H K'} \quad (7)$$

Taking the logarithm of Eq. (7) we now have a means of determining the association number,  $N$ , in dilute basic solution, if  $\text{TiO}_2$  does indeed form a weak acid in solution as we have assumed, for

$$\log \text{TiO}_{(2+n)}^{-2n} = \log K_H K' + 2n \log \text{OH}^- \quad (8)$$

In Fig. (7) the molar concentration of  $\text{TiO}_2$  is plotted against the molar concentration of  $\text{NaOH}$ .<sup>†</sup> The slopes of the curves between 0.1 and 1N  $\text{NaOH}$  are essentially the same within experimental error. The values of 2.6 - 2.8, at first sight, would indicate that species such as  $\text{H}_4\text{TiO}_4$  and  $\text{H}_2\text{TiO}_3$  are being formed, for  $n = 1.3 - 1.4$ . However, X-ray analysis of the precipitates from the 1.0 N  $\text{NaOH}$  solutions have shown that  $\text{Na}_2\text{O} \cdot 3\text{TiO}_2$  and  $\text{Na}_2\text{O} \cdot 5\text{TiO}_2$  were produced at this concentration. Formation of these compounds would have a dominating effect on the slopes of the curves and their presence would prohibit resolution of the question without additional data. To resolve the problem requires measurement of solubility in basic solution by the sampling method.

<sup>†</sup> For this part of the discussion only, it was assumed that all  $\text{TiO}_2$ , measured by the weight loss of the crystals, was present in solution in the form of some titanate such as  $\text{TiO}_3^{=}$ ,  $\text{TiO}_4^{-4}$ , etc.

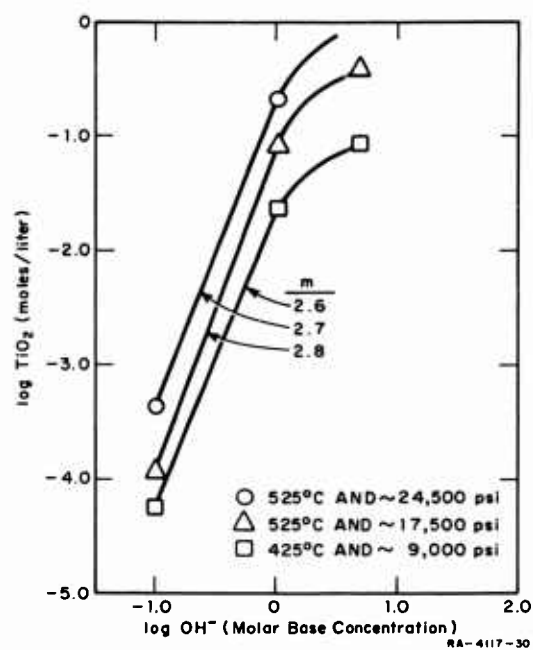
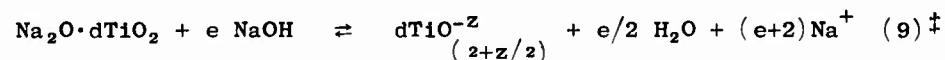


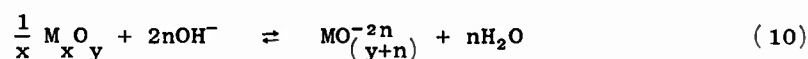
FIG. 7 APPARENT MOLAR SOLUBILITY  
 DEPENDENCE OF RUTILE (see footnote on  
 preceding page) ON BASE CONCENTRATION  
 AT CONSTANT TEMPERATURE AND  
 NEARLY CONSTANT PRESSURE

A comparison with Lux's<sup>26</sup> results for the system  $\text{Na}_2\text{O}-\text{TiO}_2$  at  $950^\circ\text{C}$  shows a striking similarity. At very low  $\text{Na}_2\text{O}$  concentration  $\text{TiO}_2$  did not react, but with increasing  $\text{Na}_2\text{O}$  concentration  $\text{Na}_2\text{Ti}_5\text{O}_{11}$  was formed: this species yielded to  $\text{Na}_2\text{O}\cdot 3\text{TiO}_2$  upon the addition of more  $\text{Na}_2\text{O}$ . Lower titanates were produced at higher sodium oxide concentrations. If the behavior is the same for the system  $\text{TiO}_2-\text{NaOH}-\text{H}_2\text{O}$  then the general equation



should describe the solution process in any range of  $\text{NaOH}$  concentration where a singular species predominates and a plot of Eq. (8), as applied to (9) will produce a linear representation in the region of stability of the species, for  $\frac{e}{d} = 2n$ .

If we now extend Eqs. (8) and (9) to other oxides in basic solution the following general equations may be applied:



and

$$\log \text{M}_x \text{O}_y = \frac{2n}{x} \log \text{AOH} + C \quad (11)$$

where  $\text{AOH}$  represents any of the alkali hydroxides. Equation (11) is general and applies to all cases obeying Eq. (10), including reactions of the nature of those represented by Eq. (9).

Equation (11) has been applied to the solubility data of Newkirk and Smith<sup>15</sup> for  $\text{BeO}$ ; Laudise and Kolb's<sup>13</sup> data for  $\text{ZnO}$ ; and Barnes, Laudise, and Shields'<sup>14</sup> results on  $\text{Al}_2\text{O}_3$ . Graphical representation of those results are shown in Figs. (8a) and (8b). The slope of 1 for  $\text{Al}_2\text{O}_3$  confirms Barnes, Laudise, and Shields reported mechanism of solution;

---

$^\dagger z = 2\left(\frac{1}{2}e + 1\right)$

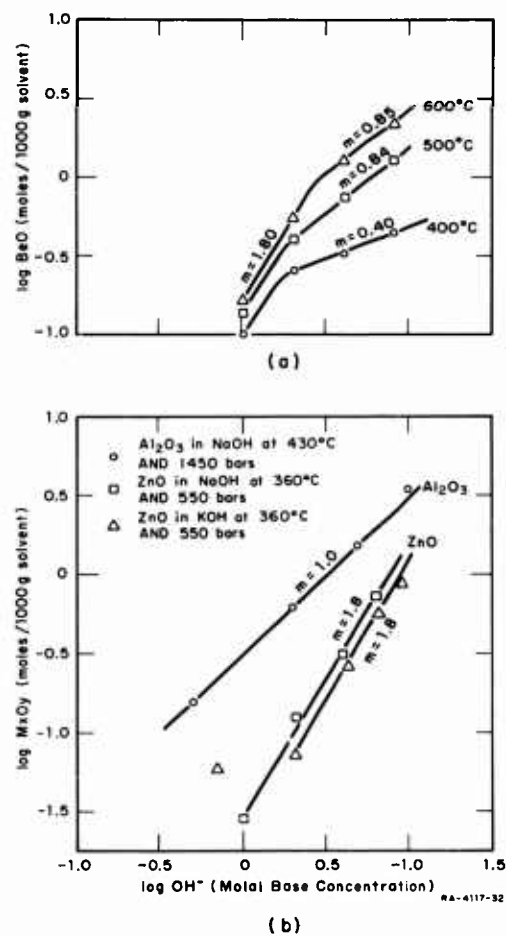
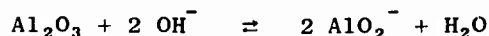
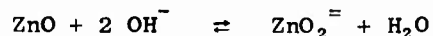


FIG. 8 SOLUBILITY DEPENDENCE OF METAL OXIDES ON BASE CONCENTRATION OF SOLVENT AT CONSTANT TEMPERATURE FOR: a) BeO after Newkirk and Smith, b) Al<sub>2</sub>O<sub>3</sub> after Barns, Laudise and Shields and ZnO after Laudise and Kolb

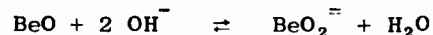
namely



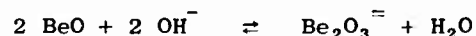
Again for  $\text{ZnO}$ , the slope of 1.8 or  $\sim 2$  is normal for the reaction



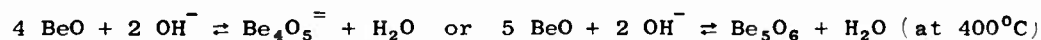
However,  $\text{BeO}$  appears to proceed by a mechanism similar to:



in normal basic solution and by the apparent mechanism:



and



in strong basic hydrothermal solution.

In any event, a linear relationship does exist on the log-log plot of solute versus base concentration in the region where a single species predominates in solution; the slope changing with the nature of the species. This relationship is temperature-dependent and probably pressure-dependent in cases where solubility is affected by pressure.

From the metal oxides whose solubilities have been investigated extensively, it can be concluded that in general the extent of solubility in water is insufficient to produce crystal growth at a reasonable rate and that recourse to growth from basic solution is desirable and in most cases necessary. Since a linear relationship between solubility and base concentration does exist, combined with the fact that the Van't Hoff equation is generally applicable for the temperature dependence of solubility, it is possible to calculate from a minimum of measurements one of the primary factors affecting hydrothermal crystal growth; namely, the region where solubility and supersaturation are sufficient to produce growth. Actually from these relationships a minimum of four solubility measurements at two base concentrations (between 2 and 10 molar) and two temperatures, at constant pressure, can give a reasonable estimate of the solubility of a given compound in the supercritical region of water from  $400^\circ$  to  $600^\circ\text{C}$  and in some cases beyond this. This assumes, of course, one phase and one species for the oxide.

Van't Hoff's equation,  $\frac{d \ln S}{dT} = \frac{\Delta H}{RT^2}$ , has been applied to rutile at two base concentrations and at two different pressures. The adherence of the data to this equation is illustrated in Fig. (9). The following

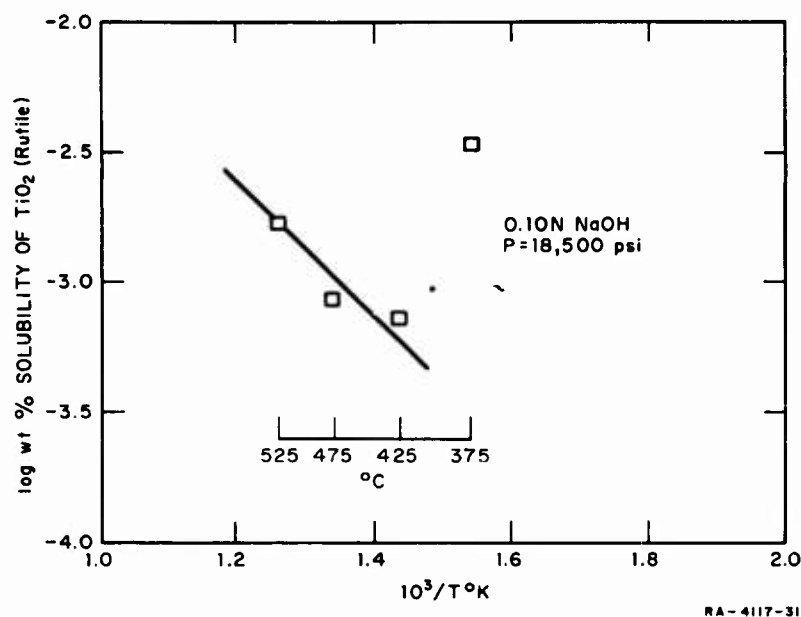


FIG. 9 OBSERVED TEMPERATURE EFFECT OF SOLUBILITY FOR RUTILE SYSTEM AT NEARLY CONSTANT PRESSURE

heat of solution was calculated from the graph:

$$0.1 \text{ N NaOH} \quad \text{and} \quad \bar{P} = 18,500 \text{ psi}, \quad \Delta H \simeq 12 \text{ kcal/mole}$$

A  $\Delta H$  of 28 kcal/mole was calculated for  $\text{TiO}_2$  in 1 N NaOH at 16,000 psi. The uncertainty as to the nature of the solution at this concentration, however, makes this value questionable.

A difference in the heats of solution between 0.1 N and 1 N NaOH would be expected for different species formation. However, the values

appear high as well as the divergence for the two solutions. These apparently anomalous values can be indicative of the scatter in the data, or that the weight loss technique for measuring solubilities is not suitable for rutile because of the titanate formation in stronger basic solution.

#### ACKNOWLEDGMENTS

We wish to thank the people who have contributed to this project in varying capacities:

Dr. William J. Fredericks who conceived the original goal of the program and initiated and directed the work before assuming his duties as Professor of Chemistry at Oregon State University

Dr. David S. Bloom, Chairman of the Solid State Physics Department for his interest, guidance, and review of the research effort

Dr. Ferenc E. Rosztoczy, Physical Chemist, for the lively discussions which were ever fruitful in helping to resolve many of the problems encountered

Mr. Kenyon Borg, Senior Technician, for the detailed design and construction of the furnaces and supplementary mechanical apparatus; also for his valuable aid in putting the high pressure vessels into working condition and keeping the laboratory equipment in operating order

Mr. John Lindsay, Chemist, for performing many of the experiments during a time when experimental difficulties seemed insurmountable

Mr. John Saunders and Mr. Oliver Smith who provided the X-ray and quantitative analysis of the samples.

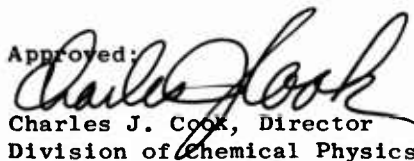


W. J. Silva, Project Leader



R. C. Smith, Jr.

Approved:



Charles J. Cook, Director  
Division of Chemical Physics

# REFERENCES

1. Laudise, R. A. and R. A. Sullivan, Chem. Eng. Progr. 55, No. 5, 55-9 (1959).
2. Laudise, R. A. and A. A. Ballman, J. Phys. Chem. 64, 688 (1960).
3. Laudise, R. A. and A. A. Ballman, J. Am. Chem. Soc. 80, 2655-7 (1958).
4. Laudise, R. A., "Hydrothermal Synthesis of Single Crystals," in Progress in Inorganic Chemistry," Vol. III, edited by F. A. Cotton, Interscience, New York, 1962, p. 1 ff.
5. Morey, G. W. and J. M. Hesselgesser, Trans ASME 73, 865-75 (1951).
6. Kennedy, G. C., Econ, Geol. 39, 25-31 (1944).
7. Laudise, R. . and A. A. Ballman, J. Phys. Chem. 66, 1396 (1961).
8. Sourirajan, S. and G. C. Kennedy, Am. J. Sci. 260, 115-141 (1962).
9. Copeland, C. S., J. Silverman, and S. W. Benson, J. Chem. Phys. 21, No. 1, 12-16 (1953).
10. Ölander, A. and H. Liander, Acta Chem. Scandinavica 4, 1437 (1950).
11. Franck, E. U., Z. physik Chem. 8, 92-106 (1956).
12. Franck, E. U., Z. physik Chem. 8, 192-206 (1956).
13. Laudise, R. A. and E. D. Kolb, Amer. Mineral. 48, 642 (1963).
14. Barns, R. L., R. A. Laudise and R. M. Shields, J. Phys. Chem. 67, 835 (1963).
15. Newkirk, H. W. and D. K. Smith, University of California, Lawrence Radiation Laboratory, Report No. UCRL-7466, August (1963).
16. Kennedy, G. C., Am. J. Sci. 257, 563-73 (1959).
17. Morey, G. W. and J. M. Hesselgesser, Econ. Geol. 46, 821 (1951).
18. Holser, W. T. and G. C. Kennedy, Am. J. Sci. 256, 744-53 (1958).
19. Holser, W. T. and G. C. Kennedy, Am. J. Sci. 257, 71-77 (1959).
20. Pauling, L., "The Nature of the Chemical Bond," 3rd Edition, Cornell University Press, Ithaca, N. Y. 1960, p. 559.
21. Roy, D. M., R. Roy and E. F. Osborn, Am. J. Sci. 251, 337-61 (1953).
22. MacDonald, G. J. F., J. Geol. 63, 244-252 (1955).
23. Kennedy, G. C., Am. J. Sci. 254, 567-73 (1956).
24. Roy, D. M. and R. Roy, Am. J. Sci. 255, 573-82 (1957).
25. Franck, E. U., Z. physik Chem. 6, 345-55 (1956).
26. Lux, Von Hermann, Zeit. fur Elektrochemie 53, 45-47 (1959).



DISTRIBUTION  
LIST A

<u>Code</u>	<u>Organization</u>	<u>No. of Copies</u>
AF 5	AFMTC (AFMTC Tech Library - MU-135 Patrick AFB, Fla.  AFMTC (MTBAT) Patrick AFB, Fla.	1
AF 18	AUL Maxwell AFB, Ala.	1
AF 32	OAR (RROS, Col. John R. Fowler) Tempo D 4th and Independence Avenue Wash. 25, D. C.	1
AF 33	AFOSR, OAR (SRYP) Tempo D 4th and Independence Avenue Wash. 25, D. C.	1
AF 43	ASD (ASNRR) Wright-Patterson AFB, Ohio	1
AF 124	RADC (RAALD) Attn: Documents Library Griffiss AFB, New York	1
AF 139	AF Missile Development Center (MDGRT) Holloman AFB, New Mexico	1
AF 314	Hq. OAR (RRY) Attn: James A. Fava, Col. USAF Wash. 25, D. C.	1
Ar 5	Commanding General USASRDL Ft. Monmouth, New Jersey Attn: Tech. Doc. Ctr. SIGRA/SL-ADT	1
Ar 9	Department of the Army Office of the Chief Signal Officer Wash. 25, D. C. Attn: SIGRD-4a-2	1
Ar 50	Commanding Officer Attn: ORDTL-012 Diamond Ordnance Fuze Laboratories Wash. 25, D. C.	1

List A - Page 2

<u>Code</u>	<u>Organization</u>	<u>No. of Copies</u>
Ar 67	Redstone Scientific Information Center U. S. Army Missile Command Redstone Arsenal, Alabama	1
G 2	Defense Documentation Center (DDC) Cameron Station Alexandria, Virginia	20
G 31	Office of Scientific Intelligence Central Intelligence Agency 2430 E Street, N.W. Wash. 25, D. C.	1
G 68	Scientific and Technical Information Facility Attn: NASA Representative (S-AK-DL) P. O. Box 5700 Bethesda, Maryland	1
G 109	Director Langley Research Center National Aeronautics and Space Administration Langley Field, Virginia	1
M 6	AFCRL, OAR (CRXRA - Stop 39) L. G. Hanscom Field Bedford, Mass.	20
M 77	Hq. AFCRL, OAR (CRTE, M. B. Gilbert) L. G. Hanscom Field, Bedford, Mass.	1
M 83	Hq. AFCRL, OAR (CRTPM) L. G. Hanscom Field, Bedford, Mass.	1
N 9	Chief, Bureau of Naval Weapons Department of the Navy Washington 25, D. C. Attn: DLI-31	2
N 29	Director (Code 2027) U. S. Naval Research Laboratory Washington 25, D. C.	2
I 292	Director, USAF Project RAND The Rand Corporation 1700 Main Street Santa Monica, California THRU: AF Liaison Office	1

List A - Page 3

<u>Code</u>	<u>Organization</u>	<u>No. of Copies</u>
U 443	Institute of Science and Technology The University of Michigan Post Office Box 618 Ann Arbor, Michigan Attn: BAMIRAC Library	1
AF 318	Aero Res. Lab. (OAR) AROL Lib. AFL 2292, Bldg. 450 Wright-Patterson AFB, Ohio	1
Ar 107	U. S. Army Aviation Human Research Unit U. S. Continental Army Command P. O. Box 428, Fort Rucker, Alabama Attn: Maj. Arne H. Eliasson	1
G 8	Library Boulder Laboratories National Bureau of Standards Boulder, Colorado	2
M 63	Institute of the Aerospace Sciences, Inc. 2 East 64th Street New York 21, New York Attn: Librarian	1
M 84	AFCRL, OAR (CRXR, J. R. Marple) L. G. Hanscom Field, Bedford, Mass.	1
N 73	Office of Naval Research Branch Office, London Navy 100, Box 39 F. P. O. New York, New York	5
U 32	Massachusetts Institute of Technology Research Laboratory Building 26, Room 327 Cambridge 39, Mass. Attn: John H. Hewitt	1
U 431	Alderman Library University of Virginia Charlottesville, Virginia	1
G 6	Scientific Information Officer British Defence Staffs Defence Research Staff British Embassy 3100 Massachusetts Avenue, N. W. Washington 8, D. C.	3

(Technical/Scientific reports will be released for military purposes only and any proprietary rights which may be involved are protected by US/UK Government agreements.)

List A - Page 4

<u>Code</u>	<u>Organization</u>	<u>No. of Copies</u>
G 9	Defence Research Member Canadian Joint Staff 2450 Massachusetts Avenue, N. W. Washington 8, D. C. (Technical/scientific reports will be released for military purposes only and any proprietary rights which may be involved are protected by US/Canadian Government Agreements.)	3

# DISTRIBUTION

## LIST R

<u>Code</u>	<u>Organization</u>	<u>No. of Copies</u>
AF 137	ASD (ASRNEM, Mr. Richard Alberts) Wright-Patterson AFB, Ohio	1
Ar 83	USASRDL Attn: SIGRA/SL-PD, H. Jacobs Fort Monmouth, New Jersey	1
G 70	Advisory Group on Electron Devices (AGED) Office of the Director of Defense Research & Engineering 346 Broadway, 8th Floor New York 13, New York	4
I 44	Bell Telephone Laboratories, Inc. Murray Hill, New Jersey Attn: Dr. J. Early	1
I 979	Radio Corporation of America RCA Laboratories Princeton, New Jersey Attn: Dr. William Webster	
N 2	Chief, Bureau of Ships Department of the Navy Attn: Mr. A. H. Young, Code 681A1A Washington 25, D. C.	1
U 269	Stanford Electronics Laboratories Stanford University Stanford, California Attn: Dr. John G. Linville	1
	Philips Laboratories Division of North American Philips Co., Inc. Irvington on Hudson, New York Attn: R. C. Bohlinger	1
	Hq. AFCRL, OAR (CRWPC) L. G. Hanscom Field Bedford, Mass.	7

**STANFORD  
RESEARCH  
INSTITUTE**

**MENLO PARK  
CALIFORNIA**

### **Regional Offices and Laboratories**

#### **Southern California Laboratories**

820 Mission Street  
South Pasadena, California

#### **Washington Office**

808-17th Street, N.W.  
Washington 6, D.C.

#### **New York Office**

270 Park Avenue, Room 1770  
New York 17, New York

#### **Detroit Office**

1025 East Maple Road  
Birmingham, Michigan

#### **European Office**

Pelikanstrasse 37  
Zurich 1, Switzerland

#### **Japan Office**

c/o Nomura Securities Co., Ltd.  
1-1 Nihonbashidori, Chuo-ku  
Tokyo, Japan

### **Representatives**

#### **Toronto, Ontario, Canada**

Cyril A. Ing  
Room 710, 67 Yonge St.  
Toronto 1, Ontario, Canada

#### **Milan, Italy**

Lorenzo Franceschini  
Via Macedonio Melloni, 49  
Milano, Italy